Photocatalytic low-temperature defluorination of PFASs

https://doi.org/10.1038/s41586-024-08179-1

Received: 11 January 2024

Accepted: 8 October 2024

Published online: 20 November 2024

Check for updates

Hao Zhang[1], Jin-Xiang Chen[1], Jian-Ping Qu[2]✉ & Yan-Biao Kang[1]✉

Polyfluoroalkyl and perfluoroalkyl substances (PFASs) are found in many everyday consumer products, often because of their high thermal and chemical stabilities, as well as their hydrophobic and oleophobic properties[1]. However, the inert carbon–fluorine (C–F) bonds that give PFASs their properties also provide resistance to decomposition through defluorination, leading to long-term persistence in the environment, as well as in the human body, raising substantial safety and health concerns[1–5]. Despite recent advances in non-incineration approaches for the destruction of functionalized PFASs, processes for the recycling of perfluorocarbons (PFCs) as well as polymeric PFASs such as polytetrafluoroethylene (PTFE) are limited to methods that use either elevated temperatures or strong reducing reagents. Here we report the defluorination of PFASs with a highly twisted carbazole-cored super-photoreductant **KQGZ**. A series of PFASs could be defluorinated photocatalytically at 40–60 °C. PTFE gave amorphous carbon and fluoride salts as the major products. Oligomeric PFASs such as PFCs, perfluorooctane sulfonic acid (PFOS), polyfluorooctanoic acid (PFOA) and derivatives give carbonate, formate, oxalate and trifluoroacetate as the defluorinated products. This allows for the recycling of fluorine in PFASs as inorganic fluoride salt. The mechanistic investigation reveals the difference in reaction behaviour and product components for PTFE and oligomeric PFASs. This work opens a window for the low-temperature photoreductive defluorination of the ‘forever chemicals’ PFASs, especially for PTFE, as well as the discovery of new super-photoreductants.

Polyfluoroalkyl and perfluoroalkyl substance (PFAS) structure–activity relationships and degradation mechanisms have been extensively investigated with hydrated electrons by ultraviolet light irradiation[6–9]. Other PFAS degradation pathways have also been documented by means of hydrothermal[10], mechanochemical[11], electrochemical[12] and plasma[13] methods, as well as heterogeneous[14] or homogeneous catalysis[15] or base-assisted decomposition[16]. As one of the best known and widely applied PFASs, polytetrafluoroethylene (PTFE) is extremely inert towards decomposition and cannot be recovered by the normal plastics recycling methods[17,18]; it can even tolerate 260 °C for years. Pyrolysis of PTFE usually proceeded over 500 °C (refs. 19–21). Breakage of the carbon–fluorine bond was also known in the combustion of metal fluorocarbon pyrolants, which have found applications in military and civilian pyrotechnics[22]. Defluorination of PTFE at low temperature (<100 °C) required extremely strong reducing agents, such as alkali-metal naphthalides[23,24], alkali or alkali-earth metals in liquid ammonia[25], benzoin dianion[26,27], lithium and sodium amalgams[28], magnesium(I) complex[29] and so on.

Defluorination of PTFE

A photoreductant is a chemical species that can be excited by absorbing light and transfers an electron from its excited state to another organic molecule, which then undergoes a reduction process. We started the PTFE defluorination using a range of photoreductants[30], in which KF was assigned as the fluoride product and its yield was determined by ^{19}F nuclear magnetic resonance (NMR) analysis (Supplementary Figs. 1–24 and Supplementary Tables 1–10). When typical metal-based photoreductants (for detailed structures, see Supplementary Table 9) with excited oxidative potential ($^*E_{ox}$) from −0.81 V to −1.73 V versus saturated calomel electrode (SCE) were subjected to the model reaction conditions, no conversion was observed (Fig. 1a). Typical organic photoreductants with $^*E_{ox}$ from −1.12 V to −3.00 V (versus SCE) gave ≤18% yield. The emergence of super-photoreductants, usually with $^*E_{ox}$ lower than −3.00 V, may provide an opportunity for the reductive cleavage of inert C–F bonds in PTFE. However, **CBZ4** (−3.13 V versus SCE), **DBPP** (−3.16 V versus SCE[31]), **DCA** (−3.20 V versus SCE[32]), **ITh** anion (−3.38 V versus SCE[33]), **BPTZ** anion (−3.51 V versus SCE[34]) and **Mes-Acr-(^{t}Bu)Ph$^+$** (radical form, −3.36 V versus SCE for the TICT model[35]) gave no improvement. **BPI** (radical anion form, $^*E_{ox}$ −2.43 to −4.28 V by density functional theory calculations[36]) gave 31% yield. The mechanistic insight of different types of photocatalyst (PC) in the photoreduction such as dehalogenation and Birch reduction has been discussed in previous reports[33]. When the twisted carbazole-cored **CBZ5** ($^*E_{ox}$ = −2.91 V versus SCE) and **CBZ6** ($^*E_{ox}$ = −2.16 V versus SCE)[37–39] was used, 55–56% yields

[1]Hefei National Research Center for Physical Sciences at the Microscale, Department of Chemistry, University of Science and Technology of China, Hefei, China. [2]Institute of Advanced Synthesis, School of Chemistry and Molecular Engineering, Nanjing Tech University, Nanjing, China. ✉e-mail: ias_jpqu@njtech.edu.cn; ybkang@ustc.edu.cn

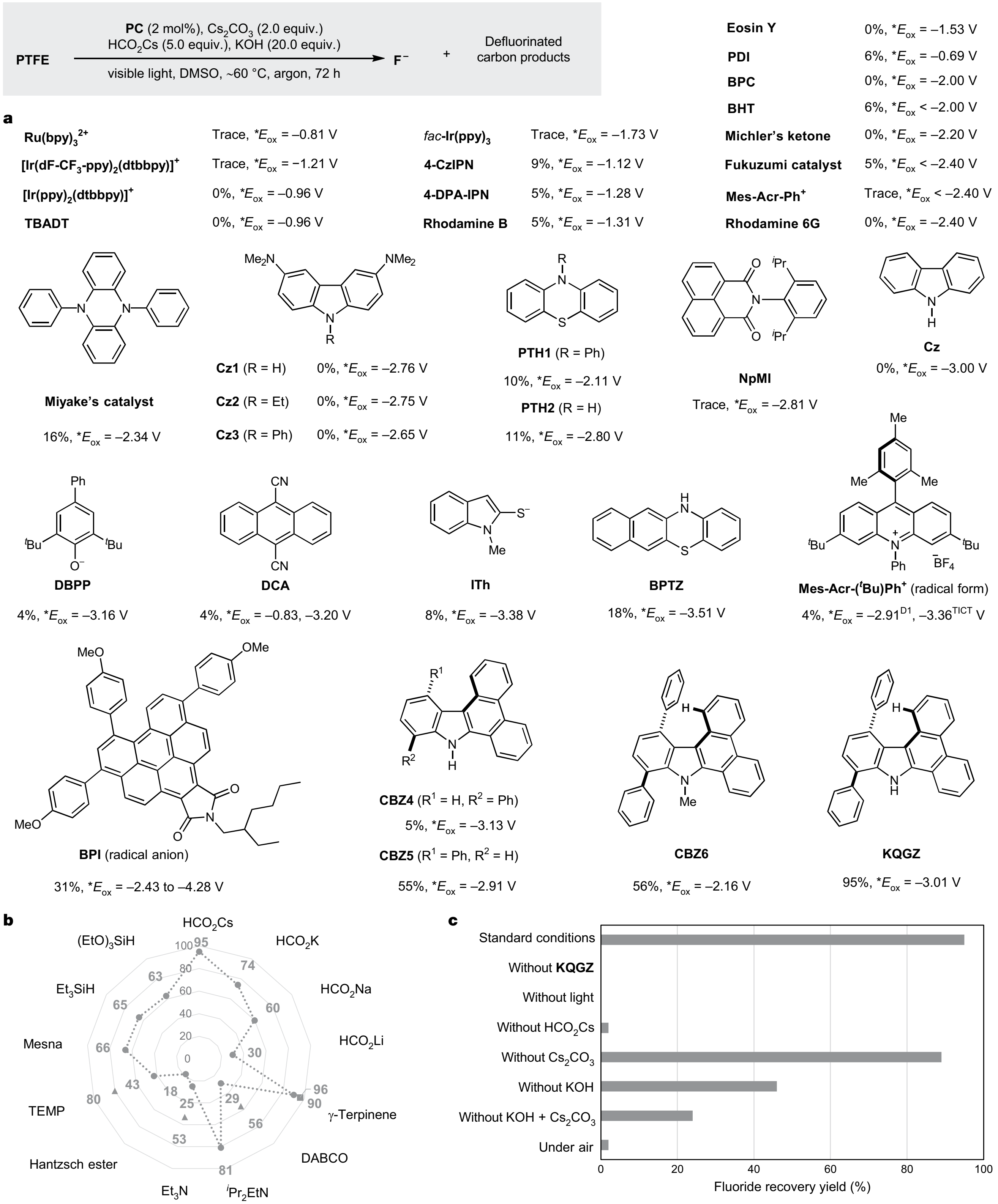

Fig. 1 | Photocatalytic reductive defluorination of PTFE. Standard conditions: photocatalyst (2 mol%), Cs_2CO_3 (2.0 equiv.), HCO_2Cs (5.0 equiv.), KOH (20.0 equiv.), 407-nm LED (54 W), DMSO, about 60 °C, argon, 72 h. Note that both the reported optimized wavelength and the 407-nm LED were tested for each PC (see Supplementary Tables 9–15 for details). **a**, Effects of photocatalysts under standard conditions. Note that the reaction mixture turned black during the course of defluorination because of the production of the amorphous carbon product; no or slight colour changes were observed when other PCs were used. **b**, Effects of reducing reagents (electron donors) under standard conditions. The grey dots represent yields obtained by means of variation of the reducing reagents under standard conditions, the grey triangles represent yields obtained by adding n-$C_{12}H_{25}SH$ (20 mol%) and the grey square represents the yield obtained by using γ-terpinene (10.0 equiv.) without caesium formate and caesium carbonate for 48 h. **c**, Control experiments under standard conditions. The grey bars represent the fluoride recovery yield. DABCO, 1,4-diaza-bicyclo[2.2.2]octane; Mesna, sodium 2-mercaptoethane sulfonate; TEMP, 2,2,6,6-tetramethylpiperidine.

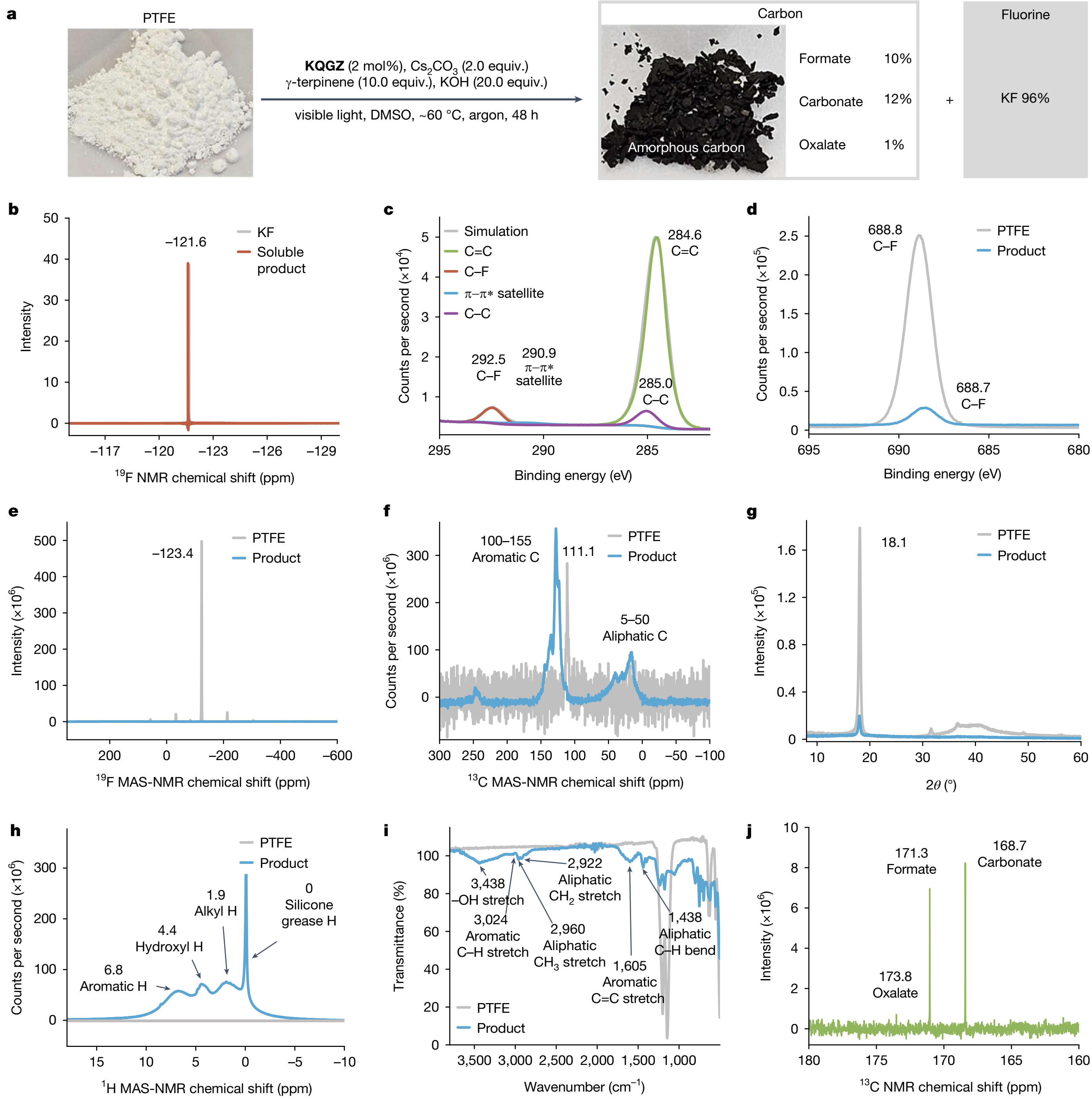

Fig. 2 | Characterization and quantification of the PTFE defluorination products. Reaction conditions: **KQGZ** (2 mol%), γ-terpinene (10.0 equiv.), KOH (20.0 equiv.), 407-nm LED (54 W), DMSO, about 60 °C, argon, 48 h. **a**, Defluorination reaction conditions. **b**, ^{19}F NMR of products and KF. **c**, C(1*s*) XPS profile of carbon product. **d**, F(1*s*) XPS profile of PTFE and carbon product. **e**, ^{19}F MAS-NMR of carbon product and PTFE. **f**, ^{13}C MAS-NMR of PTFE and carbon product. **g**, Powder X-ray diffraction of PTFE and carbon product. **h**, ^{1}H MAS-NMR of PTFE and carbon product. **i**, ATR-IR of PTFE and carbon product. **j**, ^{13}C NMR of the minor carbon products.

were achieved. Encouraged by the results of **CBZ6**, a more electron-rich photoreductant **KQGZ**$^-$ ($^*E_{ox}$ = −3.01 V versus SCE) in situ generated by the deprotonation of **KQGZ** (−2.06 V versus SCE) was then tested and 95% yield was obtained. However, simple carbazoles (**Cz**, −3.00 V versus SCE; **Cz1**–**Cz3**, about −2.76 to −2.65 V versus SCE[40]) were inefficient for the defluorination of PTFE. The photocatalytic reduction ability shows no direct dependence on the value of $^*E_{ox}$ of a PC.

A variety of common reducing reagents, such as silanes[15], formates, amines and so on, were investigated; most of the reducing reagents demonstrated good reactivity (Fig. 1b and Supplementary Table 11). γ-Terpinene[33] and caesium formate[41] gave the highest yields. In the case of DABCO, Et_3N and TEMP[42], an increased yield was observed when 20 mol% thiol was added[41,43].

Control experiments confirm the necessity of light, photocatalyst and reducing reagent (Fig. 1c and Supplementary Table 8). KOH is important for a high yield, whereas the reaction without KOH gave a moderate yield. The reaction can also proceed in other solvents, such as DMF, DMA, NMP, THF and DMSO-H_2O (Supplementary Table 12).

			F (mol%)		C (mol%)				
a Entry	Molecular structure	Abbreviation	Fluoride	Trifluoroacetate	Formate	Carbonate	Oxalate	Trifluoroacetate	Tartronate
1[a]	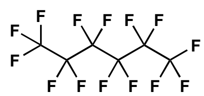	**PFHx**	82.0 ± 4.5	11.0 ± 6.6	–	–	–	–	–
			81.4 ± 2.5 (83.3)	7.2 ± 0.9 (5.6)	(33.3)	(37.9)	(9.2)	(8.7)	–
2[b]	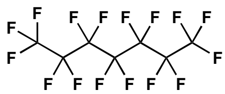	**PFHp**	87.7 ± 3.7	12.2 ± 4.2	–	–	–	–	–
			85.3 ± 2.8 (91.4)	10.7 ± 1.7 (7.6)	(35.0)	(42.9)	(5.4)	(11.6)	–
3[c]	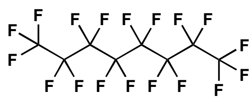	**PFO**	81.0 ± 5.1	9.0 ± 4.8	–	–	–	–	–
			80.3 ± 2.2 (82.8)	6.7 ± 1.3 (5.3)	(24.4)	(46.6)	(6.3)	(7.9)	–
4[b]	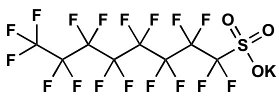	**PFOS**	92.0 ± 3.0	15.0 ± 6.0	–	–	–	–	–
			90.4 ± 3.7 (93.5)	8.2 ± 2.3 (6.1)	(27.8)	(28.1)	(12.8)	(8.7)	(10.8)
5[b]	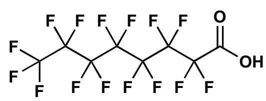	**PFOA**	89.0 ± 5.7	12.3 ± 5.7	–	–	–	–	–
			90.3 ± 1.5 (93.1)	8.9 ± 2.1 (6.0)	(25.3)	(28.1)	(20.0)	(7.5)	–
6[b]	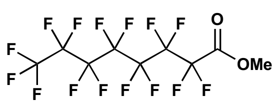	**PFOE**	86.3 ± 4.3	10.7 ± 4.3	–	–	–	–	–
			87.8 ± 1.9 (91.1)	6.7 ± 0.8 (4.9)	(17.5)	(30.6)	(17.8)	(6.1)	–
7[b,d]	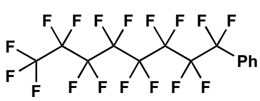	**PFOB**	77.7 ± 2.7	11.0 ± 3.7	–	–	–	–	–
			91.2 ± 3.3 (94.1)	5.8 ± 1.1 (3.6)	(29.7)	(20.3)	(21.9)	(5.1)	(9.4)

b

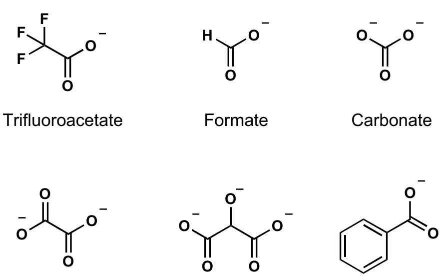

c

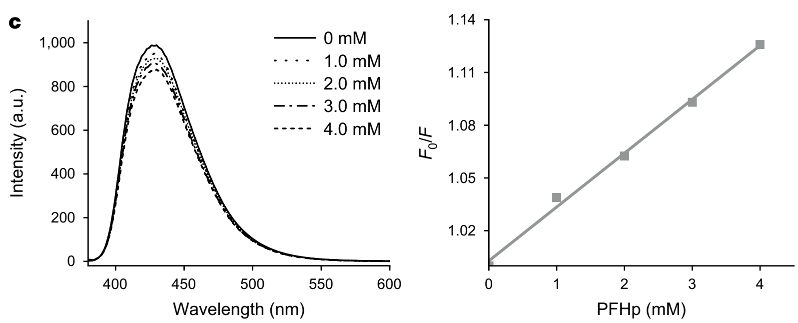

Fig. 3 | Investigations on the defluorination of PFASs. a, Defluorination of PFASs. Upper rows use the conditions stated in Fig. 1a for 24 h and yields are determined by IC analysis. Lower rows use the conditions stated in Fig. 2a for 24 h and yields are determined by IC analysis. Yields in parentheses are determined by ^{19}F or ^{13}C NMR analysis. **b**, Structures of anionic carbon-containing products. **c**, Fluorescence quenching effects of PFHp with **KQGZ** and the Stern–Volmer plot. [a]HCO_2Cs (8.0 equiv.), DMSO/deionized water (2 ml/0.25 ml), 48 h or 36 h in the case of γ-terpinene. [b]24 h. [c]HCO_2Cs (10.0 equiv.), DMSO/deionized water (2 ml/0.25 ml), 48 h or 36 h in the case of γ-terpinene. [d]10.6% of benzoate was observed through ^{13}C NMR analysis. a.u., arbitrary units.

Also, no reaction occurred under thermal conditions (Supplementary Table 8 and Supplementary Fig. 24), excluding the possible photothermal conversion process[16].

Characterization and quantification of defluorination products were performed using γ-terpinene as the reducing reagent to avoid the interference of formates and carbonates on the analysis of components of the products (Fig. 2a). Amorphous carbon (**P9** in Fig. 5a) was obtained by filtration. The F-anion in the solution was confirmed by ^{19}F NMR analysis (Fig. 2b) and 96% fluoride yield was estimated using hexafluoroisopropanol as an internal standard (Supplementary Fig. 26). The weak C–F signal in the X-ray photoelectron spectroscopy (XPS) spectrum (Fig. 2c,d), almost complete disappearance of C–F resonances in ^{19}F (δ = −123.4 ppm; Fig. 2e) and ^{13}C (δ = 111.1 ppm; Fig. 2f) solid-state magic-angle spinning (MAS)-NMR spectra and the weak intensity at 18.1° from powder X-ray diffraction analysis (Fig. 2g) of carbon product further confirmed the nearly complete cleavage of C–F bonds of PTFE.

The 77% yield of the amorphous carbon was calculated as moles of carbon in the product per mole of carbon of PTFE, containing 2% fluorine (see Supplementary Information). The peaks of the C(1*s*) XPS profile at 284.6 eV and 290.9 eV were assigned to the C=C bond and π–π* satellite, respectively (Fig. 2c). The aromatic subunits were confirmed by the peaks in the ^{13}C (100–155 ppm) and ^{1}H (around 6.8 ppm) MAS-NMR spectrum (Fig. 2f,h and Supplementary Figs. 33–36), as

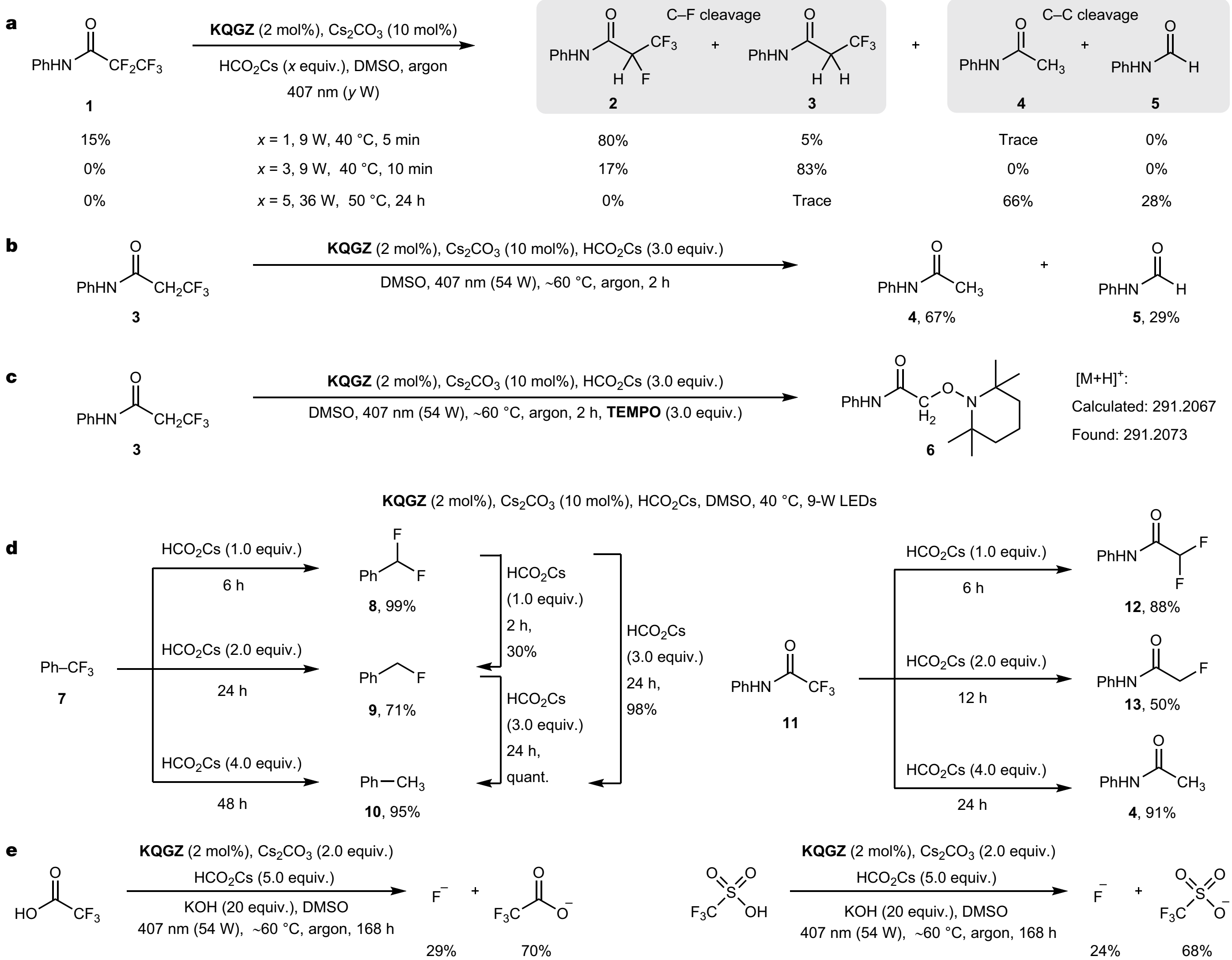

Fig. 4 | Control experiments. a, The C–F and C–C cleavage of **1**. **b**, C–C cleavage of **3**. **c**, The radical trapping by **TEMPO**. **d**, Gradient C–F cleavage of **7** and **11**. Reaction conditions: fluorinated compound (0.2 mmol, 1.0 equiv.), **KQGZ** (2 mol%), Cs_2CO_3 (10 mol%), HCO_2Cs, DMSO (1 ml), 407 nm (9 W) light, under argon atmosphere at about 40 °C. **e**, Defluorination of acids, in which the yield is calculated as moles of fluorine in the corresponding product per mole of fluorine in starting material.

well as the strong intensity at around 1,605 cm^{-1} (Fig. 2i and Supplementary Figs. 38 and 40) and the weak intensity at 3,100–3,000 cm^{-1} (Fig. 2i and Supplementary Figs. 38 and 39) in the attenuated total reflectance infrared (ATR-IR) spectroscopy analysis. The polycyclic aromatic carbon (125–137 ppm) was identified by ^{13}C MAS-NMR analysis (Supplementary Fig. 34). The peak of the C(1*s*) XPS profile at 285.0 eV (Fig. 2c), the chemical shift at 5–50 ppm in the ^{13}C MAS-NMR spectrum (Fig. 2f and Supplementary Fig. 35) and at around 1.9 ppm in the ^{1}H MAS-NMR spectrum (Fig. 2h) corresponded to the C–C single bond. The chemical shift at around 4.4 ppm in the ^{1}H MAS-NMR spectrum (Fig. 2h) and the wavenumber around 3,438 cm^{-1} in the ATR-IR spectroscopy analysis (Fig. 2i) were assigned to the hydroxyl hydrogen. Combustion experiments of the amorphous carbon product showed that it sustained smouldering and remained red-hot without any flame in the presence of continuous heating under air[44] (Supplementary Fig. 44 and Supplementary Video 1). It should be noted that the quantitative inverse-gated-decoupling ^{1}H-decoupled ^{13}C NMR analysis of the solution shows the generation of 10% formate, 12% carbonate and 1% oxalate (Fig. 2j and Supplementary Fig. 27). Comparison of scanning electron microscopy of PTFE (Supplementary Fig. 42) and the amorphous carbon product (Supplementary Fig. 43) shows changes on the surface.

Defluorination of perfluoroalkyl substances

Perfluorocarbons (PFCs) (C_nF_{2n+2}), such as perfluorohexane (PFHx), perfluoroheptane (PFHp) and perfluorooctane (PFO), are fully fluorinated analogues of hydrocarbons. The reductive C–F cleavage of PFCs remains a challenge owing to the inert C–F bonds that result in the remarkable low reduction potentials[45]. The **KQGZ**-catalysed defluorination of PFCs proceeded smoothly to give >80% yields (by ion chromatography (IC) or ^{19}F NMR analysis) (Fig. 3a, entries 1–3, and Supplementary Figs. 45–50). Trifluoroacetate was observed as the minor fluoride product. When γ-terpinene was used as the electron donor, formate, carbonate, oxalate and trifluoroacetate were identified as the carbon-containing products by quantitative ^{13}C NMR analysis, together with compatible fluoride yields (Fig. 3b). The fluorescence quenching effects of **KQGZ** with PFHp as well as the Stern–Volmer plot prove the photocatalytic nature of this reaction (Fig. 3c and Supplementary Figs. 59 and 60).

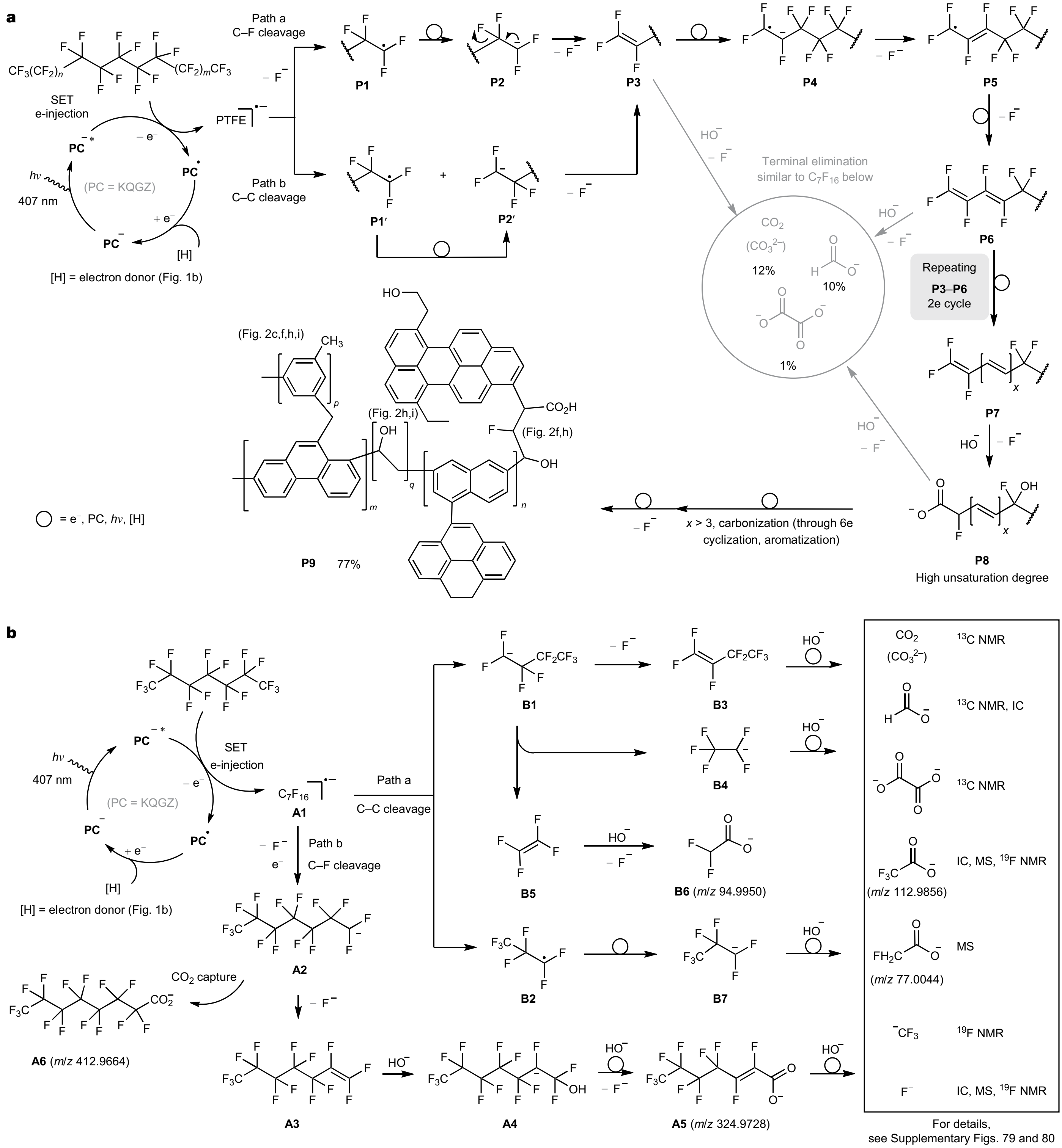

Fig. 5 | Proposed mechanism. a, The defluorination of PTFE is assumed to proceed by means of a surface reaction in which the electron transfers between **KQGZ** and the surface of PTFE. **b**, The defluorination of oligomeric PFASs is assumed to proceed in the solution or emulsion. For details, see Supplementary Figs. 79 and 80. MS, mass spectrometry.

Perfluorooctane sulfonic acid (PFOS), polyfluorooctanoic acid (PFOA) and polyfluorocarboxylic acid ester (PFOE), as well as (perfluorooctyl)benzene (PFOB), could be efficiently defluorinated (Fig. 3a, entries 4–7 and Supplementary Figs. 51–58). Fluoride and trifluoroacetate were observed as F products by IC or ^{19}F NMR analysis, whereas formate, carbonate, oxalate and trifluoroacetate were identified as C-containing products. Also, 10.8% of tartronate for PFOS and 9.4% of tartronate as well as 10.6% of benzoate for PFOB were observed.

Mechanistic investigations

In both PTFE and perfluoroalkyl substance defluorinations, photoreductive C–F and C–C bond cleavages were involved. In the case of pentafluoroamide **1**, by slightly enhancing the reaction conditions, the C–F cleavage products **2** and **3** as well as the C–C cleavage product **4** could be selectively obtained (Fig. 4a and Supplementary Figs. 61– 63). When **3** was subjected to standard conditions, C–C cleavage products **4** and **5** were obtained (Fig. 4b). The radical nature of the light-induced $C(sp^3)$–F cleavage has been reported[41,42], whereas the radical nature of the C–C cleavage of **3** was proved by the trapping experiment (Fig. 4c and Supplementary Fig. 64).

Although the light-induced defluorination of small molecules such as $PhCF_3$ **7** (refs. 41,42,46) or trifluoromethyl amide **11** are known[47,48], the complete defluorination of such molecules has barely been developed. The reason for this is that the reduction potentials of the C–F bond in trifluoromethyl groups gradually become more negative and less polar during the loss of fluorine. In this work, the C–F bonds of **7** ($E_{p/2}$ −2.50 V)[41] could be gradually cleaved by increasing the loading of electron donors and prolonging the reaction time, affording **8**–**10** in 71–99% yields (Fig. 4d and Supplementary Figs. 65–67). Complete defluorination of **8** and **9** could also be accomplished (Supplementary Figs. 68–70). In the case of **11**, the sequential defluorination could be accomplished by the same strategy to afford **12**, **13** and **4** (Fig. 4d and Supplementary Fig. 71). The defluorination of the smaller acids such as trifluoroacetic acid and triflic acid is less effective compared with the corresponding amide **11** (Fig. 4e), owing to the difficulty for the electron transfer to the C–F bond adjacent to the electron-rich carboxylate anion.

On the basis of the control experiments including the gradient bond cleavage experiments, the radical trapping experiment, the light-off experiments (Supplementary Fig. 24), the fluorescence quenching effects (Fig. 3c and Supplementary Figs. 59 and 60) and the anionic mass spectrometry analysis (Supplementary Figs. 72–77), the proposed mechanism for the photoreductive defluorination of PTFE and PFASs is illustrated in Fig. 5.

For PTFE, the single-electron transfer (SET) from photoexcited **PC*** yields PTFE radical anion, followed by two pathways (a and b) through C–C and C–F bond cleavage (Fig. 5a). In pathway a, the release of F anion gives radical **P1**, which is further converted to **P3** through SET and defluorination. **P3** is an unsaturated perfluoropolymer, which is highly electron-deficient and readily able to obtain an electron from **PC*** to form radical anion **P4**. **P4** is converted to diene **P6** by repeating defluorination and SET. The process of **P3** to **P6** passes 2e injection and defluorination twice. Repeating this 2e cycle of **P3**–**P6** yields high-unsaturated-degree perfluoropolymer **P7**. The addition–elimination of unsaturated bonds of **P7** by HO^- gives carboxylated and hydroxylated **P8**. The following cyclization/aromatization of polyene moiety of **P8** forms the aromatic units. The further carbonization affords the coal-like carbon product **P9**. (The proposed carbonization of **P8** to **P9** remains unclear and warrants further investigation. See ref. 49 on the carbonization of polyvinyl chloride.) In pathway b, the C–C bond breaks to form radical **P1′** and anion **P2′**. **P1′** can be further reduced to anion **P2′**, followed by the defluorination to unsaturated polymer **P3**. The transformation of **P3** to **P9** is same as in pathway a. Owing to the insolubility of PTFE in the solvent, the electron transfer from **PC*** to PTFE takes place on the surface of PTFE. After carbonization, the carbon product releases from the polymer with the aid of stirring and the photoreduction could continue. When γ-terpinene was used as the electron donor, besides carbon and KF, carbonate and carboxylates including carbonate (from CO_2), formate, trifluoroacetate and oxalate were also detected by ^{13}C NMR, IC, electrospray ionization mass spectrometry or ^{19}F NMR. These salts were generated through the elimination on the terminals of **P7** and **P8** aided by KOH through a similar process as C_7F_{16} shown in Fig. 5b.

The mechanism for the reaction of oligomeric PFASs is similar to that of PTFE, except their products are small-molecule salts rather than amorphous carbon. This might result from the good solubility (for PFOS and PFOA) or dispersity (C6–C8 perfluoroalkanes, PFOE and PFOB) in the solvent. Using PFHp as the model molecule, the mechanism for the reaction of oligomeric PFASs is demonstrated in Fig. 5b. The electron injection from **PC*** to C_7F_{16} affords radical anion **A1**. Either C–F or C–C bond cleavage is possible, whereas the C–F bond cleavage is before the C–C bond. For the longer chains of perfluoroalkanes, the C–C bonds can be further polarized and the competing C–C and C–F bonds' reductive cleavage affords C_7F_{15} anion ($C_7H_{15}^-$, **A2**), C_4F_9 anion ($C_4H_9^-$, **B1**) and C_3F_7 radical ($C_3H_7^{\cdot}$, **B2**). The C_3F_7 radical is reduced to C_3F_7 anion ($C_3H_7^-$, **B7**). These anions pass through F elimination to form alkenes such as **B3** and **A3** (ref. 16). The formation of radical through C–F reductive elimination is supported by the control experiments in Fig. 4c. When γ-terpinene[33] is used as the electron donor, anion **A2** can capture CO_2 to form **A6** (ref. 50), in which CO_2 is in situ generated[16]. In the presence of KOH, the nucleophilic addition of HO^- to the double bonds of **A3** or **B3** was followed by the F elimination to yield carboxylic anions[16] (*m*/*z* 94.9950; *m*/*z* 325). Repeating the above process yields the final fragmentation products.

Conclusions

We report a twisted carbazole-cored **KQGZ** as an organic superphotoreductant for reductive defluorination/degradation of a range of PFASs. By comparison of the carbazole-cored PCs such as **Cz**, **CBZ4**, **CBZ5**, **CBZ6** and **KQGZ**, the electron-transfer ability could be related to the torsion of the carbazole ring. The comparison of a wide range of reported photoreductants in this work indicates that excited oxidation potentials ($^*E_{ox}$) are not the only standard for the photoreduction ability.

Online content

Any methods, additional references, Nature Portfolio reporting summaries, source data, extended data, supplementary information, acknowledgements, peer review information; details of author contributions and competing interests; and statements of data and code availability are available at https://doi.org/10.1038/s41586-024-08179-1.

1. Evich, M. G. et al. Per- and polyfluoroalkyl substances in the environment. *Science* **375**, eabg9065 (2022).
2. Washington, J. W. et al. Nontargeted mass-spectral detection of chloroperfluoropolyether carboxylates in New Jersey soils. *Science* **368**, 1103–1107 (2020).
3. Singh, K., Kumar, N., Yadav, A. K., Singh, R. & Kumar, K. Per- and polyfluoroalkyl substances (PFAS) as a health hazard: current state of knowledge and strategies in environmental settings across Asia and future perspectives. *Chem. Eng. J.* **475**, 145065 (2023).
4. Sunderland, E. M. et al. A review of the pathways of human exposure to poly- and perfluoroalkyl substances (PFASs) and present understanding of health effects. *J. Expo. Sci. Environ. Epidemiol.* **29**, 131–147 (2019).
5. Gaballah, S. et al. Evaluation of developmental toxicity, developmental neurotoxicity, and tissue dose in zebrafish exposed to GenX and other PFAS. *Environ. Health Perspect.* **128**, 047005 (2020).
6. Bentel, M. J. et al. Defluorination of per- and polyfluoroalkyl substances (PFASs) with hydrated electrons: structural dependence and implications to PFAS remediation and management. *Environ. Sci. Technol.* **53**, 3718–3728 (2019).
7. Bentel, M. J. et al. Degradation of perfluoroalkyl ether carboxylic acids with hydrated electrons: structure–reactivity relationships and environmental implications. *Environ. Sci. Technol.* **54**, 2489–2499 (2020).
8. Liu, Z. et al. Accelerated degradation of perfluorosulfonates and perfluorocarboxylates by UV/sulfite + iodide: reaction mechanisms and system efficiencies. *Environ. Sci. Technol.* **56**, 3699–3709 (2022).
9. Gao, J. et al. Photochemical degradation pathways and near-complete defluorination of chlorinated polyfluoroalkyl substances. *Nat. Water* **1**, 381–390 (2023).
10. Hao, S. et al. Hydrothermal alkaline treatment for destruction of per- and polyfluoroalkyl substances in aqueous film-forming foam. *Environ. Sci. Technol.* **55**, 3283–3295 (2021).
11. Yang, N. et al. Solvent-free nonthermal destruction of PFAS chemicals and PFAS in sediment by piezoelectric ball milling. *Environ. Sci. Technol. Lett.* **10**, 198–203 (2023).
12. Schaefer, C. E. et al. Electrochemical transformations of perfluoroalkyl acid (PFAA) precursors and PFAAs in groundwater impacted with aqueous film forming foams. *Environ. Sci. Technol.* **52**, 10689–10697 (2018).
13. Singh, R. K. et al. Rapid removal of poly- and perfluorinated compounds from investigation-derived waste (IDW) in a pilot-scale plasma reactor. *Environ. Sci. Technol.* **53**, 11375–11382 (2019).
14. Baumgartner, R., Stieger, G. K. & McNeill, K. Complete hydrodehalogenation of polyfluorinated and other polyhalogenated benzenes under mild catalytic conditions. *Environ. Sci. Technol.* **47**, 6545–6553 (2013).

15. Douvris, C. & Ozerov, O. V. Hydrodefluorination of perfluoroalkyl groups using silylium-carborane catalysts. *Science* **321**, 1188–1190 (2008).
16. Trang, B. et al. Low-temperature mineralization of perfluorocarboxylic acids. *Science* **377**, 839–845 (2022).
17. Puts, G. J., Crouse, P. & Ameduri, B. M. Polytetrafluoroethylene: synthesis and characterization of the original extreme polymer. *Chem. Rev.* **119**, 1763–1805 (2019).
18. Améduri, B. & Hori, H. Recycling and the end of life assessment of fluoropolymers: recent developments, challenges and future trends. *Chem. Soc. Rev.* **52**, 4208–4247 (2023).
19. Yang, X. et al. A chemical route from PTFE to amorphous carbon nanospheres in supercritical water. *Chem. Commun*. 342–343 (2004).
20. Simon, C. M. & Kaminsky, W. Chemical recycling of polytetrafluoroethylene by pyrolysis. *Polym. Degrad. Stab.* **62**, 1–7 (1998).
21. Ellis, D. A., Mabury, S. A., Martin, J. W. & Muir, D. C. G. Thermolysis of fluoropolymers as a potential source of halogenated organic acids in the environment. *Nature* **412**, 321–324 (2001).
22. Koch, E.-C. *Metal-Fluorocarbon Based Energetic Materials* (Wiley, 2011).
23. Nelson, E., Kilduff, T. J. & Benderly, A. A. Bonding of Teflon. *Ind. Eng. Chem.* **50**, 329–330 (1958).
24. Yoshino, K. et al. Conducting polymer prepared from teflon. *Jpn. J. Appl. Phys.* **21**, L301–L302 (1982).
25. Chakrabarti, N. & Jacobus, J. The chemical reduction of poly(tetrafluoroethylene). *Macromolecules* **21**, 3011–3014 (1988).
26. Costello, C. A. & McCarthy, T. J. Surface modification of poly(tetrafluoroethylene) with benzoin dianion. *Macromolecules* **17**, 2940–2942 (1984).
27. Costello, C. A. & McCarthy, T. J. Surface-selective introduction of specific functionalities onto poly(tetrafluoroethylene). *Macromolecules* **20**, 2819–2828 (1987).
28. Kavan, L., Dousek, F. P., Janda, P. & Weber, J. Carbonization of highly oriented poly(tetrafluoroethylene). *Chem. Mater.* **11**, 329–335 (1999).
29. Sheldon, D. J., Parr, J. M. & Crimmin, M. R. Room temperature defluorination of poly(tetrafluoroethylene) by a magnesium reagent. *J. Am. Chem. Soc.* **145**, 10486–10490 (2023).
30. Wu, Y., Kim, D. & Teets, T. S. Photophysical properties and redox potentials of photosensitizers for organic photoredox transformations. *Synlett* **33**, 1154–1179 (2022).
31. Liang, K. et al. Intermolecular oxyarylation of olefins with aryl halides and TEMPOH catalyzed by the phenolate anion under visible light. *Chem. Sci.* **11**, 6996–7002 (2020).
32. Kim, H., Kim, H., Lambert, T. H. & Lin, S. Reductive electrophotocatalysis: merging electricity and light to achieve extreme reduction potential. *J. Am. Chem. Soc.* **142**, 2087–2092 (2020).
33. Wu, S., Schiel, F. & Melchiorre, P. A general light-driven organocatalytic platform for the activation of inert substrates. *Angew. Chem. Int. Ed.* **62**, e202306364 (2023).
34. Halder, S., Mandal, S., Kundu, A., Mandal, B. & Adhikari, D. Super-reducing behavior of benzo[*b*]phenothiazine anion under visible-light photoredox condition. *J. Am. Chem. Soc.* **145**, 22403–22412 (2023).
35. MacKenzie, I. A. et al. Discovery and characterization of an acridine radical photoreductant. *Nature* **580**, 76–81 (2020).
36. Cole, J. P. et al. Organocatalyzed birch reduction driven by visible light. *J. Am. Chem. Soc.* **142**, 13573–13581 (2020).
37. Xiao, Z. F. et al. Iridium-catalyzed cyclization of isoxazolines and alkenes: divergent access to pyrrolidines, pyrroles, and carbazoles. *Org. Lett.* **18**, 5672–5675 (2016).
38. Luan, Z. H., Qu, J. P. & Kang, Y. B. Discovery of oxygen α-nucleophilic addition to α,β-unsaturated amides catalyzed by redox-neutral organic photoreductant. *J. Am. Chem. Soc.* **142**, 20942–20947 (2020).
39. Wang, S. D., Yang, B., Zhang, H., Qu, J. P. & Kang, Y. B. Reductive cleavage of C–X or N–S bonds catalyzed by super organoreductant CBZ6. *Org. Lett.* **25**, 816–820 (2023).
40. Yabuta, T., Hayashi, M. & Matsubara, R. Photocatalytic reductive C–O bond cleavage of alkyl aryl ethers by using carbazole catalysts with cesium carbonate. *J. Org. Chem.* **86**, 2545–2555 (2021).
41. Sap, J. B. I. et al. Organophotoredox hydrodefluorination of trifluoromethylarenes with translational applicability to drug discovery. *J. Am. Chem. Soc.* **142**, 9181–9187 (2020).
42. Chen, K., Berg, N., Gschwind, R. & König, B. Selective single C(sp3)–F bond cleavage in trifluoromethylarenes: merging visible-light catalysis with Lewis acid activation. *J. Am. Chem. Soc.* **139**, 18444–18447 (2017).
43. Wang, H. & Jui, N. T. Catalytic defluoroalkylation of trifluoromethylaromatics with unactivated alkenes. *J. Am. Chem. Soc.* **140**, 163–166 (2018).
44. Picheau, E., Amar, S., Derré, A., Pénicaud, A. & Hof, F. An introduction to the combustion of carbon materials. *Chem. Eur. J.* **28**, e202200117 (2022).
45. Patrick, J. S., Pradeep, T., Luo, H., Ma, S. & Cooks, R. G. Gas-phase C-F bond cleavage in perfluorohexane using W-, Si-, P-, Br-, and I-containing ions: comparisons with reactions at fluorocarbon surfaces. *J. Am. Soc. Mass. Spectrom.* **9**, 1158–1167 (1998).
46. Vogt, D. B., Seath, C. P., Wang, H. & Jui, N. T. Selective C–F functionalization of unactivated trifluoromethylarenes. *J. Am. Chem. Soc.* **141**, 13203–13211 (2019).
47. Campbell, M. W. et al. Photochemical C–F activation enables defluorinative alkylation of trifluoroacetates and -acetamides. *J. Am. Chem. Soc.* **143**, 19648–19654 (2021).
48. Ye, J. H., Bellotti, P., Heusel, C. & Glorius, F. Photoredox-catalyzed defluorinative functionalizations of polyfluorinated aliphatic amides and esters. *Angew. Chem. Int. Ed.* **61**, e202115456 (2022).
49. Nagai, Y., Smith, R. L.Jr., Inomata, H. & Arai, K. Direct observation of polyvinylchloride degradation in water at temperatures up to 500°C and at pressures up to 700 MPa. *J. Appl. Polym. Sci.* **106**, 1075–1086 (2007).
50. Campbell, S. F., Stephens, R. & Tatlow, J. C. Perfluorocycloalkenyl-lithium compounds. *Chem. Commun.* 151–152 (1967).

Data availability

All data are available in the main text or the supplementary materials.

Acknowledgements This paper is dedicated to Yong Tang at Shanghai institute of Organic Chemistry on the occasion of his 60th birthday. We appreciate the financial support from the National Key R&D Program of China (no. 2021YFA1500100) and the National Natural Science Foundation of China (22271268). We thank Q. Li at the University of Science and Technology of China for assistance with the X-ray photoelectron spectroscopy measurements and characterizations. We thank K. Gong at the University of Science and Technology of China for helpful discussions about solid-state magic-angle spinning nuclear magnetic resonance characterizations.

Author contributions H.Z. performed all experiments and analysed the data in the main text and supplementary information, with guidance from Y.-B.K. and J.-P.Q., unless otherwise stated. J.-X.C. assisted H.Z., synthesized the photocatalyst shown in Fig. 1 and performed the reactions in Fig. 4a,b and the analysis. Y.-B.K. and J.-P.Q. conceived the research, designed the experiments, supervised experiments and analyses, interpreted the data, generated figures and wrote the manuscript.

Competing interests A patent application has been filed by the University of Science and Technology of China on photocatalytic defluorination of polyfluoroalkyl and perfluoroalkyl substances.

Additional information

Supplementary information The online version contains supplementary material available at https://doi.org/10.1038/s41586-024-08179-1.

Correspondence and requests for materials should be addressed to Jian-Ping Qu or Yan-Biao Kang.

Peer review information *Nature* thanks Jinyong Liu and the other, anonymous, reviewer(s) for their contribution to the peer review of this work.